4-21-2009

Static and Dynamic Responsive Behavior of Polyelectrolyte Brushes under External Electrical Field

Hui Ouyang
The University Of Akron

Zhenhai Xia
The University of Akron

Jiang Zhe
University of Akron Main Campus, jzhe@uakron.edu

Static and dynamic responses of polyelectrolyte brushes under external electric field

2009 Nanotechnology 20 195703

(http://iopscience.iop.org/0957-4484/20/19/195703)

Nanotechnology **20** (2009) 195703 (7pp) doi:10.1088/0957-4484/20/19/195703

Static and dynamic responses of polyelectrolyte brushes under external electric field

Hui Ouyang, Zhenhai Xia and Jiang Zhe[1]

Department of Mechanical Engineering, The University of Akron, 302 Buchtel Common, Akron, OH 44325-3903, USA

E-mail: jzhe@uakron.edu

Received 6 January 2009, in final form 20 March 2009
Published 21 April 2009
Online at stacks.iop.org/Nano/20/195703

Abstract
The static and dynamic behaviors of partially charged and end-grafted polyelectrolyte brushes in response to electric fields were investigated by means of molecular dynamics simulation. The results show that the polymer brushes can be partially or fully stretched by applying an external electric field. Moreover, the brushes can switch reversibly from collapsed to stretched states, fully responding to the AC electric stimuli, and the gating response frequency can reach a few hundred MHz. The effects of the grafting density, the charge fraction of the brushes and the strength of the electric field on the average height of the polymer brushes were studied through the simulations.

1. Introduction

Integrated micro/nanofluidic devices are being developed for next generation bioanalytical devices for detection and quantification of a variety of important biological targets from bacteria, virus, to DNA sequencing. One of the most important issues for these 'lab-on-a-chip' developments to go from laboratory to field applications is the development of high density parallel 'smart' sensing channels that are necessary to handle the number of samples for each testing in a reasonable time. The key to realize smart sensing channels is the use of gating elements to dynamically modulate the electrical signals of each channel, enabling signal multiplexation and demultiplexation. High throughput, low power consumption devices can thus be developed. Grafted polyelectrolyte brushes, with many remarkable features due to the electrostatic coupling between polymeric monomers and counterions, are promising for a new class of advanced gating systems for many application including high throughput nanofluidic devices, drug delivery, bioimplants, data storage, and smart valves. The polymer brushes are soluble in water at neutral pH and display strong interactions with solvents, electrolytes, and between polymer chains. They also display rich supramolecular switching behaviors under chemical and physical perturbations. By adjusting molecular structures and compositions, the polymer brushes can possess unique properties in response to external stimuli such as electric potential [1–4], temperature variation [5–7], pH alteration [8], and light [9, 10]. In the application of micro/nanofluidic devices, polyelectrolyte brushes can be grown onto the inner side of the nanofluidic channels as smart nanoactuators, where dynamic modulation of the electrical signals is achieved through expansion–collapse transitions of tethered polymer brushes in response to the changes in electrical field and fluidic conditions.

Theoretical work, including self-consistent methods [15, 16], molecular dynamics [11–14], Monte Carlo simulation [15, 16], and scaling theory [17, 18], has been carried out in recent years to predict the morphology of the brushes and the interaction between the brushes and counterions. The theoretical work and simulations are very useful to understand the relationship between the morphology and properties of the polymer brushes. Most work is, however, focused on the basic features and equilibrium structures.

Electric fields, which can be applied faster than other stimuli, represent a favorite approach to induce motion and deformation of polyelectrolytes brushes (charged polymers) and to probe their structure and properties. For gating applications, dynamic expansion–collapse of the brush under electric stimuli would result in a structure far from equilibrium state [19]. Therefore, a fundamental understanding of the

[1] Author to whom any correspondence should be addressed.

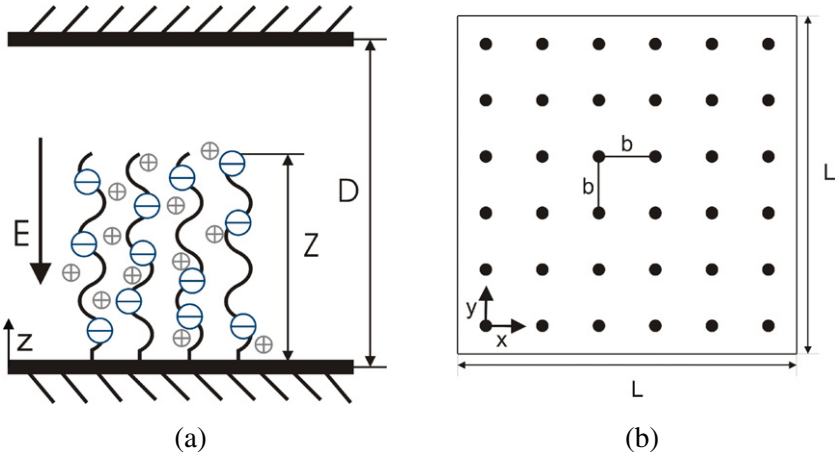

Figure 1. The schematic configuration of the polymer brushes in a nanofluidic channel; (a) the cross section view, (b) the top view; each dot represents a polyelectrolyte chain. Arrow E indicates the direction of an external electric field.

dynamic behavior of the polyelectrolytes is critical to gating mechanism, design optimization and device performance. Although some work has been done on highly charged polyelectrolyte chains in an electric field by Brownian dynamics simulation methods and a combination of different scaling arguments [20, 21], there is no systematic research on dynamic behavior of the polymer brushes with different grafting density, charge fraction, and electric field strength in micro/nanofluidic channels.

In this paper, molecular dynamics simulation was conducted for polyelectrolytes in nanofluidic channels, to predict its static and dynamic behavior in response to an electrical field. The height of polyelectrolytes grafted on a planar channel wall was simulated at various conditions. The results show that the average height of charged polymer brushes can be adjusted as much as 300% by controlling the grafting density, charge fraction and external electric field. The electric field-induced structural transition is reversible: the stretch-collapse switching can repeatedly be realized by turning the electric field on and off. The response frequency is remarkably high, up to a few hundred MHz. This work thus provides a direction to optimize the structures of polymer brushes for the design of efficient gating systems for nanofluidic devices.

2. Model and method

Molecular dynamics simulation of polyelectrolyte brushes was performed with explicit counterions. The LAMMPS package [22] was employed to conduct the simulation work, in which Ewald method was implemented with an estimated accuracy of 10^{-4}. We use the similar simulation parameters as studied by Hehmeyer *et al* [12]. In the simulation, we use coarse-grained bead-spring to represent the flexible polymer brushes which are tethered on a planar solid surface with an uncharged monomer. Such coarse grain model has been widely used to study the structures and properties of the polymer brushes [11–14]. The simulation was carried out in a constant number of particles, volume, and energy (NVE) ensemble. Periodic boundary conditions are applied only in x- and y-directions. Polymer brushes are grafted at a planar wall surface ($z = 0$) as shown in figure 1. The motion of bead i at position $\boldsymbol{r}_i(t)$ is described by Langevin equation,

$$m\frac{\mathrm{d}^2\boldsymbol{r}_i}{\mathrm{d}t^2} = -\nabla_i U_{\text{total}} - m\Gamma\frac{\mathrm{d}\boldsymbol{r}_i}{\mathrm{d}t} + \boldsymbol{W}_i(t) \tag{1}$$

where Γ is a friction constant which couples the beads to a heat bath and all the beads carry the same mass m, and $\boldsymbol{W}_i(t)$ is Gaussian random force of the heat bath acting on each beads, with

$$\langle \boldsymbol{W}_i(t)\rangle = 0, \qquad \langle \boldsymbol{W}_i(t)\cdot\boldsymbol{W}_j(t')\rangle = 6mk_{\mathrm{B}}T\Gamma\delta_{ij}\delta(t-t') \tag{2}$$

where the coupling to Γ is a consequence of the fluctuation-dissipation relation.

The potential energy, U_{total}, of the system consists of Lennard-Jones potential U_{LJ}, long-range Coulomb potential U_{coul}, a bonding potential U_{bond}, wall potential U_{wall} and electric potential U_{elec} caused by the external electric field.

$$U_{\text{total}} = U_{\text{LJ}} + U_{\text{coul}} + U_{\text{bond}} + U_{\text{wall}} + U_{\text{elec}}. \tag{3}$$

The short-range Lennard-Jones (LJ) potential, acting between any bead pair ij including monomer–monomer, monomer–counterion, and counterion–counterion is given by [12]:

$$U_{\text{LJ}}(r_{ij}) = \begin{cases} 4\varepsilon_{\text{LJ}}[(d/r_{ij})^{12} - (d/r_{ij})^{6}] & r_{ij} < r_{\text{cut}} \\ 0 & r_{ij} \geqslant r_{\text{cut}} \end{cases} \tag{4}$$

where r_{ij} is the distance between two beads, ε_{LJ} is the Lennard-Jones energy, d is the diameter of the beads including monomers and counterions, r_{cut} is the cutoff distance. We set $d = 4$ Å and the Lennard-Jones diameter $\sigma = 6.46$ Å; this gives $d = 0.62\sigma$; and $r_{\text{cut}} = 2^{1/6}d$.

Electrostatic interaction between any two charged beads separated by a distance r_{ij} is given by long-range Coulomb

potential [11]:

$$U_{\text{coul}} = \frac{e^2}{4\pi\varepsilon_0\varepsilon} \sum_{n_z=-\infty}^{\infty} \sum_{n_y=-\infty}^{\infty} \sum_{i=1}^{N_{\text{tot}}-1} \sum_{j=i+1}^{N_{\text{tot}}} \frac{q_i q_j}{|\boldsymbol{r}_{ij} + n_x L\boldsymbol{e}_x + n_y L\boldsymbol{e}_y|} \tag{5}$$

where q_i and q_j are the corresponding charges in units of elementary charge e, ε_0 is the vacuum permittivity, and ε is the dielectric constant of the solvent.

The connectivity of neighboring beads i, j in the same chain is maintained by the finite extensible nonlinear elastic (FENE) bond potential [22]:

$$U_{\text{bond}}(r_{ij}) = \begin{cases} -0.5k_{\text{spring}}R_0^2 \\ \qquad \times \log[1-(r_{ij}/R_0)^2] & r_{ij} < r_{\text{cut}} \\ \infty & r_{ij} \geqslant r_{\text{cut}} \end{cases} \tag{6}$$

with spring constant $k_{\text{spring}} = 7\varepsilon_{\text{LJ}}/\sigma^2$ and the maximum bond length $R_0 = 2.0\sigma$.

The repulsive wall potential is chosen as 12/6 Lennard-Jones potential:

$$U_{\text{wall}}(z) = \begin{cases} 4\varepsilon_{\text{LJ}}[(\sigma/z)^{12} - (\sigma/z)^6] & z < z_{\text{c}} \\ 0 & z \geqslant z_{\text{c}} \end{cases} \tag{7}$$

where z is the distance between the particle and the wall, and $z_{\text{c}} = 2^{1/6}\sigma$ is the distance from the wall at which wall–particle interaction is cut off.

An external electric field along z-direction is applied to the system. This adds a potential to each charged bead in the simulation:

$$U_{\text{elec}} = -q_i \boldsymbol{V}\boldsymbol{r}_i \tag{8}$$

where q_i is the amount of charge that ith bead carries, $\boldsymbol{V}$ is the external electric field strength in a unit of V m^{-1}, and $\boldsymbol{r}_i$ is the displacement of ith bead under the electric field. In the following simulation, we define a normalized external electric field strength, E, which is given by $E = [V(4\pi\varepsilon\varepsilon_0\sigma\varepsilon_{\text{LJ}})^{0.5}\sigma]/\varepsilon_{\text{LJ}}$.

Figure 1 shows the schematic configuration of the polymer brush–nanofluidic channel system in the simulation. The system contains a 6×6 array of tethered polyelectrolyte chains; each chain has one uncharged anchored monomer at channel wall ($z = 0$) and $N = 30$ monomers. The systems with charge fraction (f) ranging from 1/30 to 0.9 are considered, where $f = N_e/N$, and N_e is the number of negatively charged monomers per chain. To keep the solution neutral, there are $M \times N \times f$ positive free charged counterions near the charged monomers at the initial position in the solution. The grafting densities $\rho_a\sigma^2 = 0.0156$, 0.0625 and 0.12 were chosen, where the tethered points at a distance $b = (1/\rho_a)^{0.5}$ and $L = (M/\rho_a)^{0.5}$ in a unit of σ can define the simulation domain size $L \times L \times D$. The total height of the channel in z direction is $D = 40\sigma$. Two flat solid surfaces at $z = 0$ and D were generated to mimic the top and bottom repulsive walls of a fluidic channel, which define the modeling boundary in z direction. In the simulation process, we assume that the counterions do not cross the $z = 0$ and D planes.

The Bjerrum length λ_{B} of bulk water at room temperature is 7.14 Å, which is $\lambda_{\text{B}} = 1.1\sigma$ in our simulation. The temperature is set by $k_{\text{B}}T = 1.0\varepsilon_{\text{LJ}}$. While a constant temperature is assumed in this study, we note here that temperature variation, as an external stimulus, will cause expansion or collapse of brushes. Recently Jaber *et al* [7] reported that poly(*N*-isopropylacrylamide) (PNIPAM) displayed stimulus-sensitive supramolecular behaviors and exhibited change in dimension and properties with temperature variations. Temperature variation may change inter-grain interactions, which MD simulation ought to be adapted to reflect. The Langevin equation (1) is integrated using velocity-Verlet algorithm with a friction constant of $\Gamma = 1.0\tau_{\text{LJ}}^{-1}$. A time step $\delta t = 0.01\tau_{\text{LJ}}$ is used, where the Lennard-Jones time unit τ_{LJ} can be calculated by $\tau_{\text{LJ}} = (m\sigma^2/\varepsilon_{\text{LJ}})^{0.5}$. We estimate that $\tau_{\text{LJ}} \approx 100$ ps for poly(sodium styrenesulfonate) (NaPSS) with a mass of 356 000 g mol^{-1}. The external electric field along z-direction is applied after the polymer brushes reach an equilibrium state. The nondimensional E can be converted to dimensional electric strength. As an example, at $T = 300$ K if $E = 1$, the electrical field strength $V = E\varepsilon_{\text{LJ}}/[(4\pi\varepsilon\varepsilon_0\sigma\varepsilon_{\text{LJ}})^{0.5}\sigma] = \varepsilon_{\text{LJ}}^{0.5}/[(4\pi\varepsilon\varepsilon_0)^{0.5}\sigma^{1.5}] = 4.14 \times 10^7$(V m^{-1}).

The density profile and average height of polymer brushes in response to an applied electric field are our major focuses. Here we define the density of polymer brushes as the number of monomers per unit volume. The average height of polymer brushes is defined as $Z = \{\sum_{i=1}^{M}[\max(z(i))]\}/M$, which is the average of maximum values of z-coordinates of polymer brush chains. In this paper, we use normalized average height, Z/D, to present simulation results. We found that the average height and density profile remain approximately the same after 1×10^5 time steps. To ensure an equilibrium state, we considered the equilibrium state was reached at 2.5×10^5 time steps. Therefore, in the following simulations we chose to apply the electric field at 2.5×10^5 time steps.

3. Simulation results and discussion

3.1. Configurations at equilibrium states under electric field

Polymers with counterions near the charged monomers were constructed as initial configuration in a stretched state. After the polymer brushes reach their equilibrium states, an external electric field is applied in the z direction (perpendicular to the grafting surface). The equilibrium morphology and density profiles were examined after 5×10^5 time steps. Brushes displayed different configurations with different charge fraction f, grafting density, $\rho_a\sigma^2$, and external electric field strength, E. Figure 2 shows the various structures of polymer brushes with different grafting densities under external electric fields. Before applying the external electric field, the polymers are densely packed together and most counterions follow the negatively charged monomers due to the electrostatic attraction between the charged monomers and counterions (figure 2(a)).

In the presence of an external electric field applied along the z direction, the negatively charged monomers are pulled

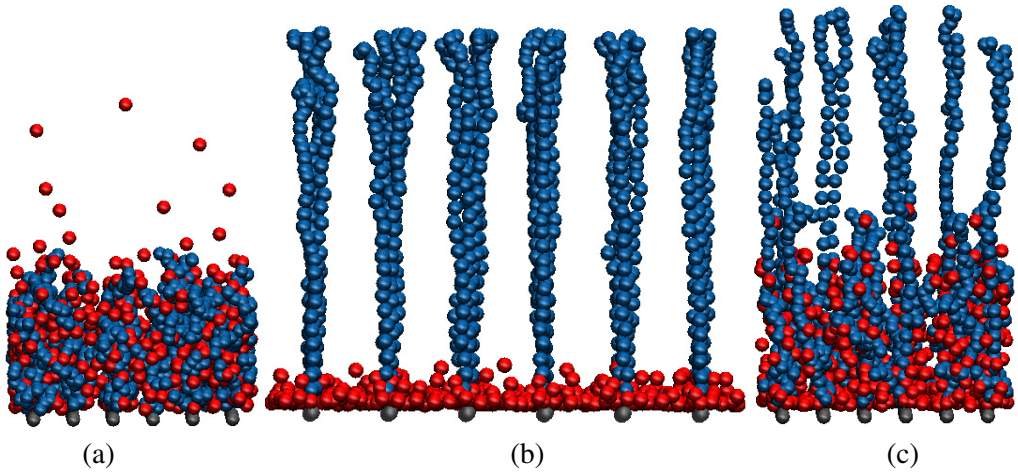

Figure 2. The snapshots of polyelectrolyte brushes simulated by molecular dynamics. Charge fraction $f = 0.5$. (a) $\rho_a\sigma^2 = 0.0625$, at equilibrium state, (b) $\rho_a\sigma^2 = 0.0156$, at $E = 3$ and (c) $\rho_a\sigma^2 = 0.0625$, at $E = 4$. The gray, blue and red spheres represent fixed monomers, free monomers and counterions.

toward the wall at $z = D$, while the positively charged counterions are driven to move towards the opposite wall. The polymer brushes can be fully stretched under the appropriate conditions. Figure 2(b) shows an example of fully-stretched polymer brushes with $f = 0.5$ and $\rho_a\sigma^2 = 0.0156$ under an electric field of $E = 3$. However, this is not the case for systems with densely grafted brushes. In those systems, not all the brushes are stretched even when a higher electric field is applied, as shown in figure 2(c). This phenomenon is attributed to the high electrostatic attractive forces between counterions and the charged monomers due to the high density of counterions and the high grafting density of polymer brushes. Because of the external electric field, the counterions become denser near the grafting wall; the Coulomb interactions between charged monomers and counterions are enhanced.

Figure 3 shows the density profiles of the polymer brushes in the presence of different electric fields. At equilibrium state, the peak density occurs at a position close to the grafting wall ($z = 0$), suggesting that most polymer brushes are packed near the wall. It is worthwhile to mention that we also simulated fully charged brushes ($f = 1$) under the same conditions as used by Hehmeyer *et al* [12]; the equilibrium morphology is consistent with their results. For densely grafted polymer brushes ($\rho_a\sigma^2 = 0.0625$), the brushes are partially stretched upon application of an electric field, resulting in an increased density away from the wall ($z > 15$) and a reduction in the peak density. The peak density still occurs near the wall indicating that the majority of counterions and polymer brushes are still trapped in a region near the grafting wall. This is due to a stronger electrostatic interaction between counterions and charged monomers, as the high density of counterions is also found near the grafting wall under the electric field. In comparison, in the case of less densely grafted polymer brushes ($\rho_a\sigma^2 = 0.0156$), the peak in the density profile disappears; all polymer chains are well stretched and monomers uniformly distribute along the z direction. This well-stretched structure can be attributed to the weaker electrostatic interaction between counterions and

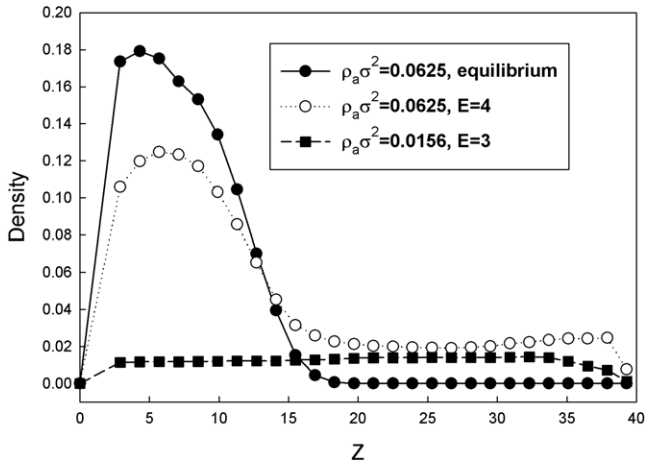

Figure 3. Density profile of polymer brushes along z direction correspond to figure 2 with $f = 0.5$.

charged monomers that can be easily overcome by the external electric field. Nearly all counterions are separated from the polymer brushes and packed near the wall ($z = 0$) under the electric field (see figure 2(b)).

The charge fraction of the polymer brushes has a significant impact on how they behave in the presence of an electric field. Simulation was done for polymer brushes with a grafting density of 0.0625; the average height of the polymer brushes was calculated as a function of charge fraction f for various electric field strengths E. The result is plotted in figure 4. In an equilibrium state (i.e., with no external electric field applied ($E = 0$)), the average height increases nearly linearly as the charge fraction increases from 0.033 to 0.9. This is because a larger charge fraction implies a larger number of charged monomers, with a proportionately larger total repulsive electrostatic interaction force between them. For an external electric field smaller than 4 ($E < 4$), the average height increases quickly with charge fraction for small charge fractions ($f \leqslant 0.2$); for larger charge fractions ($f > 0.2$),

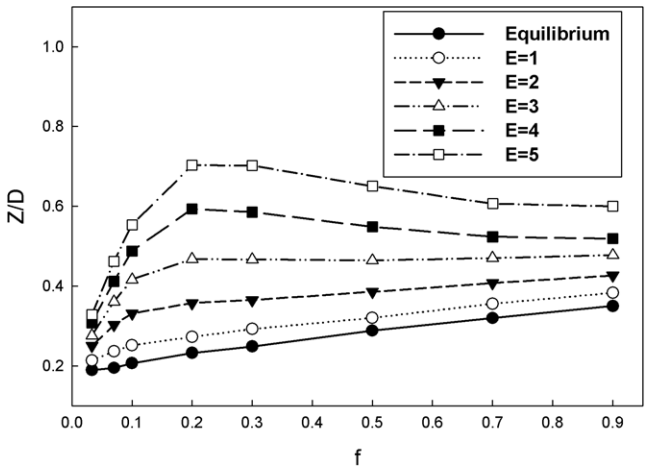

Figure 4. Average height of polymer brushes (Z/D) with grafting density $\rho_a\sigma^2 = 0.0625$ versus charge fraction f with and without electric field.

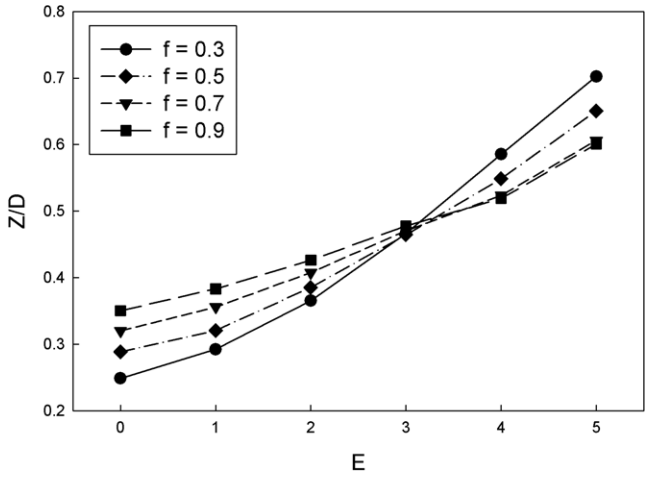

Figure 5. Average height of the monomers as a function of electric field strength for different charge fraction at grafting density $\rho_a\sigma^2 = 0.0625$.

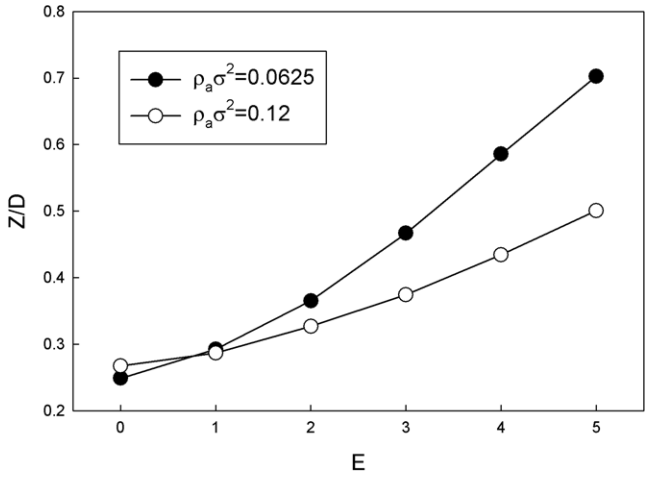

Figure 6. Average height of the polymer brushes as a function of electric field strength with different grafting density at $f = 0.3$.

the relationship is linear. In the presence of a stronger electric field ($E \geqslant 4$), the average height reaches a maximum value at $f = 0.2$, then slightly decreases, and eventually approaches a constant value (for $f > 0.7$). This can be attributed to a competition between a resisting force from the monomer–counterion interaction and a driving force from the monomer–electric field interaction. According to equation (8), the driving force on the monomer layer due to the external electric field is $F_{\mathrm{E}} = fNE$, which increases linearly with increasing charge fraction. On the other hand, when the external electric field increases, more counterions concentrate near the wall, leading to a stronger monomer–counterion interaction. For a weakly charged polymer brush, the increase in driving force due to monomer–electric field interaction is larger than the increase in resistance force due to the monomer–counterion interaction; this is what causes the sharp increase in average height at small charge fractions. When the charge fraction becomes higher, the density of counterions is increased, resulting in a larger resisting force. Once the increase in resisting force exceeds the increase in driving force, a reduction in the average height is expected. The competition between the driving force and the resisting force suggests that for partially charged polymer brushes in the presence of a strong electric field, there is a critical value of charge fraction for which the brushes are stretched maximally. For the strongly charged polymer brushes ($f > 0.7$) in the presence of a strong electric field, both the electrostatic interactions (resisting forces) and the electric field-induced force (driving force) become stronger when the charge fraction increases; the increases of the two forces are balanced. Thus, the average height remains unchanged when further increasing the charge fraction.

Figure 5 shows the average height of the monomers as a function of external electric field strength. The average height increases with increasing the electric field strength E with an increase rate dependent on the charge fraction. There is a critical value of $E = 3$, at which the charge fraction ($f \geqslant 0.2$), does not affect the average height. This is possible because for certain electric field, the enhancement of the driving force caused by increasing f, is counteracted by the increase in the resisting force. When the external electric filed is below the critical value, polymer brushes with higher charge fraction (f) show higher average height due to the stronger electric field–monomer interaction. Above the critical value, the brushes with lower charge fraction (f) show higher average height because of weaker monomer–counterion interaction. These results suggest that the average height could be controlled precisely at the critical electric field, even if the charges are non-uniformly distributed on the polymer brushes. This provides a route to minimize the variation of the average height, induced by charge non-uniformity in the fabrication of the nanochannel with polymer brushes.

The stretching of the polymer brushes with various grafting density is studied under external electric fields. As shown in figure 6, the average height increases with increasing strength of the electric field. The lower the graft density, the higher the increase rate of the average height is. This is not surprising, because at a fixed charge fraction, the driving

force remains the same; however, with a higher graft density, the interaction between monomers and counterions, i.e. the resistance force, is stronger due to higher counterions density near the wall ($z = 0$).

We note here that the change in average height of polymer brushes in response to the external electrical signals is of importance for many nanofluidic devices that require dynamic gating of electrical/fluidic impedance. In these applications, the stretched polymer brushes can be used as a functional gating element. By controlling the average height of the monomer layer, cross section area and thus flow/electrical impedance of a micro/nanochannel can be modulated. Highly stretchable polymer brushes under lower electric field are more desired for the gating applications. Considering the results in figures 1–6, polymer brushes with lower graft density and lower charge fraction have better performance in response to an external electric field. For example, the polymer with $f = 0.2$ and $\rho_a\sigma^2 = 0.0625$ can be stretched approximately 300% under an electric filed of $E = 5$, almost two times higher than highly-dense heavily charged brushes at the equilibrium state.

3.2. Dynamic responsive behavior

Dynamic response of the polymer brushes to an alternate electric field is simulated. In the simulations, a square-wave AC electric field was applied to the system after the polymer brushes reached their equilibrium state. The polymer brushes were stretched under an external electric field along z direction. When the external electric field was removed, the polymer brushes returned to their equilibrium states. The response times of the above two processes are rise time and fall time, respectively.

Figure 7 shows the dynamic behavior of the polymer brushes for a square-wave AC electric field. In figure 7(a), the electric field strength is kept as $E = 5$. To simulate the dynamic behavior of the polymer brushes, we first applied two square-waves, with a period of 2×10^5 and 1×10^5 time steps. As can be seen in figure 7(a), the polymer brushes respond to the AC electric field very well; the average height follows the square-wave shape of the applied electric field. Next, we used an electric field $E = 4$ with a high frequency (period $= 0.4 \times 10^5$ time steps). Figure 7(b) shows the dynamic average height change of polymer brushes. Rise time and fall time are calculated when the electric field is switched on and off. The rise time for different charge fractions $f = 0.1$, 0.2 and 0.7 are 10 000, 7200 and 1600 time steps; the fall time are 18 000, 15 000 and 10 000 time steps, respectively. Obviously, the response time is dependent on charge fraction f; the higher the charge fraction, the faster polymer brushes respond. Finally, an extremely high frequency (period = 20 time step) was also applied. The polymer brushes do not respond to such as high frequency electric field (not shown here). Therefore, there is a critical response frequency, below which the polymer brushes can completely follow the change of external electric field.

It is of interest to calculate the actual response frequency (in Hz) of polymer brushes, which is the reciprocal of the response time. The response frequency can be estimated for specific polymer materials. For example, for poly(sodium

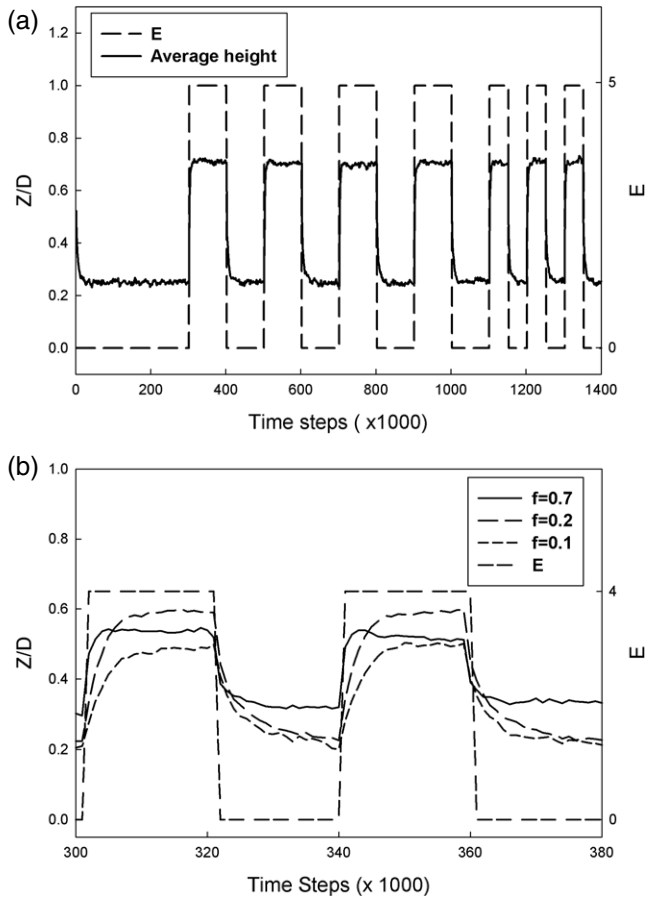

Figure 7. Average height of polymer brushes versus time steps for a system with grafting density $\rho_a\sigma^2 = 0.0625$, under a rectangle alternative electric field with (a) low frequencies with $E = 5$, $f = 0.3$, and (b) high frequency at $E = 4$, $f = 0.1$, 0.2 and 0.7.

styrenesulfonate) (NaPSS), Lennard-Jones time unit $\tau_{LJ} \approx 100$ ps, and one time step is $0.01\tau_{LJ} = 1$ ps. Then the actual response time in second can be calculated. Figure 8 shows the response frequencies converted from rise times. For lower charge fractions ($f = 0.1$ and 0.2), the critical response frequencies remain nearly constant at different electric fields, which are 100 MHz and 140 MHz respectively. For a high charge fraction ($f = 0.7$), the response frequency increases at low electric field ($E \leqslant 3$) and then reaches a stable value of approximately 435 MHz at higher electric field ($E > 3$). Similar phenomenon was also reported on free-standing polyelectrolyte that oscillates at an electric field with high frequencies (several GHz) [19]. Our result suggests that polymer brushes have excellent dynamic performance in response to the external electric stimuli and could be an effective high frequency gating system for nanofluidic devices.

4. Conclusions

The static and dynamic behavior of polymer brushes under external stimuli is important to the development of gating components for smart nanofluidic devices for many applications. We have performed molecular dynamics studies of the static and dynamic behaviors of polyelectrolyte brushes

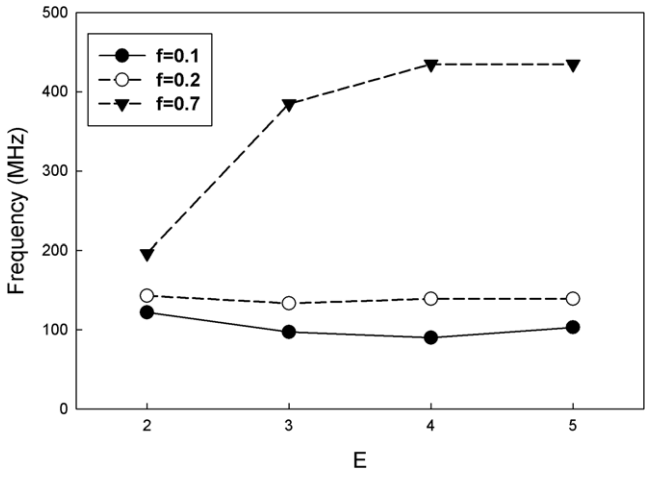

Figure 8. Response frequency (based on rise time) versus different external electric fields E at $f = 0.1$, 0.2 and 0.7 for poly(sodium styrenesulfonate) (NaPSS) polymer brushes.

grafted on a channel wall in salt-free solution under external electric field. Three types of morphologies of the polymer brushes, unstretched, partially-stretched and fully-stretched structures, were observed in the simulations.

Statically, the average stretching height of polymer brushes is affected by charge fraction, graft density of the polymer brushes, and the electric field strength. For the same charge fraction, the average stretching height increases with increasing electric field strength. Polymer brushes with low grafting density and low charge fraction display a large change in average height under external electric fields; the change could reach up to 300%, suggesting that the polymer brush nanofilm is an excellent candidate for gating systems in nanofluidic devices. Dynamically, the reversible behavior of the polymer brushes was observed when applying an AC electric field. The response frequency based on rise time of the polymer brushes can reach a few hundred MHz. The fast response to the external electric stimuli implies that the polymer brush nanofilm can be used as an effective high frequency gating component for modulating electrical/fluidic impedance in nanofluidic channels. With the polymer brushes as the gating components, it is feasible to develop advanced signal multiplexation and demultiplexation techniques that enable the next generation high throughput lab-on-a-chip devices.

Acknowledgments

This work is supported partially by the National Science Foundation under Grant Numbers ECCS-0748540 and DBI-0649798. We are grateful to Ohio Supercomputer Center (OSC) for the use of supercomputers for this work.

References

[1] Lahann J, Mitragotri S, Tran T N, Kaido H, Sundaram J, Choi I S, Hoffer S, Somorjai G A and Langer R 2003 *Science* **299** 371–4
[2] Krupenkin T N, Taylor J A, Schneider T M and Yang S 2004 *Langmuir* **20** 3824–7
[3] Abbott N L, Gorman C B and Whitesides G M 1995 *Langmuir* **11** 16–8
[4] Luk Y Y and Abbott N L 2003 *Science* **301** 623–6
[5] Lendlein A and Langer R 2002 *Science* **296** 1673–6
[6] Khongtong S and Ferguson G S 2002 *J. Am. Chem. Soc.* **124** 7254–5
[7] Jaber J A and Schlenoff J B 2005 *Macromolecules* **38** 1300–6
[8] Matthews J R, Tuncel D, Jacobs R M J, Bain C D and Anderson H L 2003 *J. Am. Chem. Soc.* **125** 6428–33
[9] Feng X, Feng L, Jin M, Zhai J, Jiang L and Zhu D 2004 *J. Am. Chem. Soc.* **126** 62–3
[10] Ichimura K, Oh S K and Nakagawa M 2000 *Science* **288** 1624–6
[11] Csajka F S and Seidel C 2000 *Macromolecules* **33** 2728–39
[12] Hehmeyer O J and Stevens M J 2005 *J. Chem. Phys.* **122** 134909
[13] Mei Y, Lauterbach K, Hoffmann M, Borisov O V, Ballauff M and Jusufi A 2006 *Phys. Rev. Lett.* **97** 158301
[14] Crozier P S and Stevens M J 2003 *J. Chem. Phys.* **118** 3855–60
[15] Chen H, Zajac R and Chakrabarti A 1996 *J. Chem. Phys.* **104** 1579–88
[16] Lai P Y and Binder K 1993 *J. Chem. Phys.* **98** 2366–75
[17] Pincus P 1991 *Macromolecules* **24** 2912–9
[18] Alexander S 1977 *J. Physique* **38** 983
[19] Netz R R 2003 *J. Phys. Chem.* B **107** 8208–17
[20] Lo T S, Khusid B, Acrivos A and Koplik J 2006 *NSTI-Nanotech.* vol 2, pp 513–6
[21] Long D, Viovy J L and Ajdari A 1996 *Phys. Rev. Lett.* **76** 3858–61
[22] Plimpton S 2005 *LAMMPS User's Manual* Sandia National Laboratory